Charge-Density-Wave Paraconductivity in $K_{0.3}MoO_3$

B. P. Gorshunov, A. A. Volkov, and G. V. Kozlov
Institute of General Physics, Russian Academy of Sciences, Vavilov Str. 38, Moscow 117942, Russia

L. Degiorgi
Laboratorium Festkörperphysik, Eidgenössische Technische Hochschule, CH-8093 Zürich, Switzerland

A. Blank, T. Csiba, M. Dressel, Y. Kim, A. Schwartz, and G. Grüner
Department of Physics and Solid State Science Center, University of California, Los Angeles, California 90024-1547
(Received 25 January 1994)

The dynamic conductivity has been measured in $K_{0.3}MoO_3$ single crystals in the conducting phase (above 180 K), for the first time over a broad frequency range 1–10^5 cm^{-1}, using a combination of different spectroscopic techniques. Together with a pseudogap, clearly pronounced excitations are observed below 50 cm^{-1} for $\vec{E} \parallel b$, the direction along which the charge density wave develops. We associate these excitations with charge-density-wave fluctuations which exist even at room temperature and give a collective contribution to the conductivity. For the transverse polarization, $\vec{E} \perp b$, a usual single-particle Drude behavior of the conductivity is observed.

PACS numbers: 71.45.Lr, 72.15.Nj

The question whether fluctuation effects lead to an increase or decrease of the conductivity above the three-dimensional (3D) ordering transition in pseudo-one-dimensional systems has been discussed ever since materials with strongly anisotropic properties were discovered [1,2]. The issue has recently been addressed again, as it has been suggested that in such materials deviations from Fermi liquid behavior may occur [3]. Clear evidence for fluctuation effects has been observed in several inorganic linear chain compounds, such as $K_{0.3}MoO_3$ and $(TaSe_4)_2I$ which develop a charge-density-wave (CDW) ground state at low temperatures. The magnetic susceptibility strongly decreases with decreasing temperature [4], suggestive of an opening of a pseudogap. Fluctuation effects well above the 3D Peierls transition have also been observed by scattering experiments [5]. Photoemission experiments [6] indicate the absence of a Fermi edge $\mathcal{E}_F$, and this is interpreted as evidence for non-Fermi liquid behavior due to one-dimensional fluctuations. In this Letter we report our experiments on $K_{0.3}MoO_3$ (blue bronze) over a broad spectral range, utilizing several novel optical configurations. We find clear evidence for the progressive opening of a pseudogap below the mean field transition temperature ($T_{MF} \approx 600$ K) but above the 3D transition ($T_{CDW} = 180$ K). Furthermore, at low frequencies we find a collective mode contribution to the conductivity, with a maximum at nonzero frequency.

All the experiments were performed on $K_{0.3}MoO_3$ single crystals prepared by the standard electrochemical method [7]. The dc conductivity measured by a four-probe technique was 2000 ± 500 $(\Omega\,cm)^{-1}$ at room temperature and increased to 3000 $(\Omega\,cm)^{-1}$ upon lowering the temperature to 200 K; the anisotropy $\sigma_\parallel/\sigma_\perp$ remains 40 at both temperatures [8].

We employed various techniques to obtain the frequency dependent conductivity $\hat{\sigma} = \sigma + i(\epsilon_\infty - \epsilon)\nu c/2$ over an extremely wide frequency range (ν is in cm^{-1} throughout the paper). In the millimeter wave frequency range a resonant cavity technique [9] was employed for surface resistance measurements. A needle shaped crystal was placed in the maximum of the electric field of a cylindrical TE_{011} cavity ($f_0 = 35.1$ GHz) and the change in width of the resonance $\Delta\Gamma$ was measured. Since

$$\frac{\Delta\Gamma}{2f_0} = \xi R_S, \tag{1}$$

the surface resistance R_S can be determined by calculating the resonator constant ξ from the geometry of the cavity and the sample [9]. We also replaced the copper end plate of a 100 GHz rectangular TE_{103} cavity by a single crystal of $K_{0.3}MoO_3$ in a configuration where the current flows along the b direction. Calibration measurements were performed by employing several metals with high dc resistivities (comparable to $K_{0.3}MoO_3$) and ξ was also calculated by numerical integration of the field distribution [9,10].

At frequencies between 8 and 36 cm^{-1}, the bulk reflectivity was measured using a quasioptical scheme of the submillimeter spectrometer "Epsilon" [11], rearranged for reflectivity measurements. The reflection coefficient was obtained by comparing the signals reflected from the sample and from a brass reference mirror, where the reflectivity of brass was calculated from the dc conductivity σ_{dc} by using the Hagen-Rubens relation:

$$R = 1 - \left(\frac{4c\nu}{\sigma_{dc}}\right)^{1/2}. \tag{2}$$

In this submillimeter (sub-mm) wave frequency range we also employed a new technique developed for direct measurements of ϵ and σ of highly reflecting samples [10,12]. The technique is based on a Fabry-Pérot res-

0031-9007/94/73(2)/308(4)$06.00

onator formed by a plane-parallel transparent dielectric plate (z-cut sapphire) and the bulk sample (with an optically flat surface of about 100 mm^2). The reflectivity spectra of the resonator, which contain sharp interference minima due to multiple reflections inside the plate, have been analyzed, and this leads directly to both ϵ and σ. Employing this technique we measured ϵ and σ of a $K_{0.3}MoO_3$ single crystal at six frequencies between 8 and 36 cm^{-1}, at two temperatures, 300 and 200 K, and for two principal orientations of $\vec{E}$ relative the conducting b axis, $\vec{E} \parallel b$ and $\vec{E} \perp b$ (i.e., $\vec{E} \parallel a$). In addition, for $\vec{E} \perp b$, a transmission measurement was performed on a specially prepared 10 μm thick sample, and the sample properties were determined from the transmitted wave amplitude and phase measurements [11]. Both types of measurements led to identical results for ϵ and for σ in the perpendicular direction.

In the optical range from 14 cm^{-1} up to 10^5 cm^{-1}, standard polarized reflection experiments ($\vec{E} \parallel b$ and $\vec{E} \perp b$) on $K_{0.3}MoO_3$ single crystals ($3 \times 2 \times 1$ mm^3) were performed by using four spectrometers. In the infrared spectral range two Fourier transform interferometers were used with a gold mirror as reference. Two grating spectrometers were employed in the visible and ultaviolet spectral ranges [7,13].

The experimental results are presented in Figs. 1–3 together with the results of dispersion analysis. In Fig. 1 the room temperature absorptivity A in both orientations is displayed as a function of frequency. The squares at 1 and 3 cm^{-1} are obtained from the measurement of the surface resistance R_S, where we have used the following relation between the absorptivity A and the surface impedance $Z_S = R_S + iX_S$:

$$A = \frac{4R_S}{Z_0}\left(1 + \frac{2R_S}{Z_0} + \frac{R_S^2 + X_S^2}{Z_0^2}\right)^{-1} \approx \frac{4R_S}{Z_0}, \qquad (3)$$

for $R_S, X_S \ll Z_0$; X_S is the surface reactance, and the free space impedance $Z_0 = 377\ \Omega$. The solid lines are the bulk reflectivity results $R = 1 - A$. The solid circles represent the results obtained using the Fabry-Pérot technique. Figure 2 shows the frequency dependent conductivity σ parallel to the b direction (300 and 200 K) and normal to the chains. In order to calculate σ from our cavity measurements (1 and 3 cm^{-1}), we assumed the Hagen-Rubens relation (2). The values of σ and ϵ in the sub-mm wave spectral range shown in Figs. 2 and 3 were obtained directly from the analysis of the Fabry-Pérot interference spectra, and independently of the reflectivity measurements. In addition to the direct measurement of the components of the optical conductivity, we have also used $A(\nu)$ over a broad frequency range to evaluate the complex conductivity. Instead of a Kramers-Kronig analysis, we used a minimum set of harmonic oscillators and Drude terms necessary to describe $A(\nu)$ as well as the conductivity and dielectric constant,

$$\hat{\sigma}(\nu) = \frac{\nu}{2ci}\sum_i \frac{\nu_{pi}^2}{\nu_{0i}^2 - \nu^2 + i\nu\gamma_i}, \qquad (4)$$

where ν_{0i}, ν_{pi}, and γ_i are the frequency, mode strength, and damping of the oscillators, respectively ($\nu_{0i} = 0$ describes a Drude term). This procedure was found to be superior to a simple Kramers-Kronig analysis of the absorptivity since the directly measured values of ϵ and σ

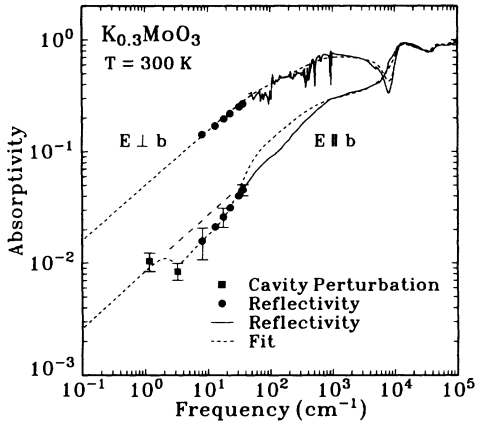

FIG. 1. Frequency dependence of the room temperature absorptivity of $K_{0.3}MoO_3$ in both orientations $\vec{E} \parallel b$ and $\vec{E} \perp b$. The squares were obtained by measuring the surface resistance, the circles represent data of quasioptical bulk reflectivity measurements. The solid lines show the optical results. The dashed lines show the results of the dispersion analysis of the data. The dot-dashed line represents the Hagen-Rubens extrapolation [Eq. (2)] as would be expected for a frequency independent conductivity.

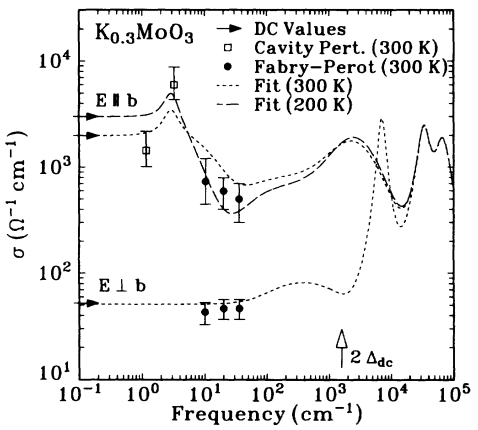

FIG. 2. Frequency dependence of the conductivity of $K_{0.3}MoO_3$ for $\vec{E} \parallel b$ (T = 300 K, 200 K) and for $\vec{E} \perp b$ (300 K). The solid circles show the result of a direct measurement of the conductivity while the lines represent the fit. The open squares are calculated from the surface impedance measurements assuming Eq. (2). The open arrow indicates the single particle gap as estimated from dc measurements below T_{CDW}.

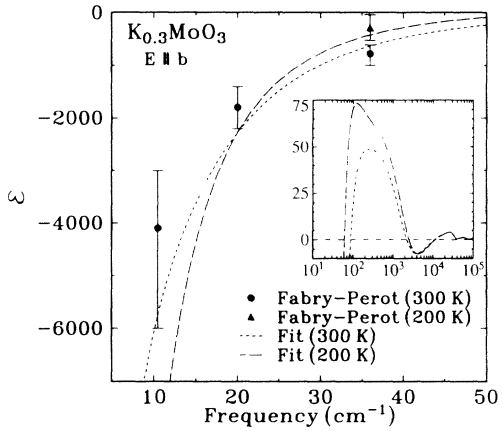

FIG. 3. The dielectric constant of $K_{0.3}MoO_3$ in the parallel direction for $T = 200$ and 300 K. The circles and triangle were obtained by direct measurements. The lines show the fit to the complete data set. In the inset the high frequency behavior and the three zero crossings of the dielectric constant can be seen.

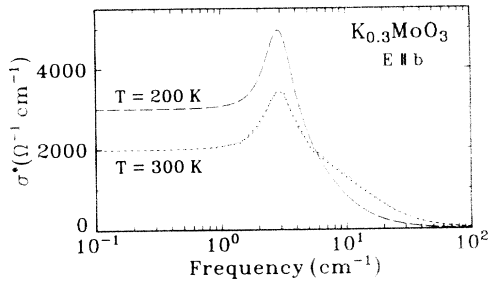

FIG. 4. The low frequency contribution to the conductivity σ^*, as described in the text.

could simultaneously be taken into account. The conductivity obtained using this procedure is shown by the dotted and the dashed lines in Fig. 2, with the dielectric constant displayed in Fig. 3. $\sigma(\nu)$ obtained in the IR range is essentially the same as found earlier [7,13,14] and will not be discussed in detail.

Next we discuss our findings. We first note that the electrodynamic response of $K_{0.3}MoO_3$ is dominated by a substantial anisotropy connected with the one-dimensional nature of the charge transport. The conductivity perpendicular to the b direction, $\sigma_\perp$, is frequency independent below 2000 cm^{-1} at room temperature. We find no dispersion in the sub-mm frequency spectra of ϵ and σ, and $\sigma_\perp(T = 300\ \mathrm{K}) \approx 50\ (\Omega\,\mathrm{cm})^{-1}$, approximately equal to its dc value [8], corresponding to the Hagen-Rubens behavior [Eq. (2)] seen in Fig. 1. The $\vec{E} \parallel b$ excitation spectra, however, show two overall features: decreasing conductivity with decreasing frequency in the far infrared range, and an enhanced conductivity at low frequencies. Assuming single particle transport for the parallel direction, $\sigma = ne^2\tau/m_b$, with $n = 5.4\times10^{21}$ cm^{-3} the electron density and $m_b = 0.9m_0$ the band mass [14], leads to $\gamma = (2\pi c\tau)^{-1} = 4500$ cm^{-1}, implying a frequency independent conductivity well below γ. In contrast, we see σ decreasing with decreasing frequency for $\nu < 1000$ cm^{-1}. Lowering the temperature enhances this feature, clearly indicating the development of a pseudogap of the same order of magnitude as the gap below the transition. The temperature dependent conductivity shows an activated behavior below T_{CDW}: $\sigma_{\mathrm{dc}} = \sigma_0 \exp(-\Delta/k_BT)$, with $2\Delta/hc \approx 1500$ cm^{-1}, in agreement with low-temperature optical data [7]; this value is indicated in Fig. 2 by the open arrow.

At low frequencies we find a pronounced enhancement of $\sigma_\parallel$ below 50 cm^{-1} (Fig. 2). This implies an additional contribution to the conductivity in the $K_{0.3}MoO_3$ spectra for $\vec{E} \parallel b$ with characteristic frequency $\nu \leq 10$ cm^{-1}. Another clear indication of this mechanism comes from the frequency dependence of ϵ in the sub-mm wave range, displayed in Fig. 3. We ascribe this contribution to the fluctuating CDW's, which gives an additional contribution σ^* to the conductivity.

The low frequency response is shown in detail in Fig. 4. This we believe is due to the fluctuating CDW response which has two important features: finite dc conductivity and a peak at 3 cm^{-1}. The latter appears at the same frequency where the pinned CDW occurs well below T_{CDW}, and we argue that it arises in the fluctuation region as well due to the interaction of the fluctuating CDW segments with impurities. In contrast to what happens in the ordered state, the fluctuating CDW segments can contribute to the dc response due to thermal fluctuations over the impurity induced barriers. The feature shown in Fig. 4 has been modeled by a harmonic oscillator and a Drude response. In the absence of final theoretical predictions it is not possible to decide whether the low frequency contribution to the conductivity is due to a single response of the collective mode, or arises due to two separate processes. Therefore we are hesitant at this moment to assign spectral weights to the composite features observed, and experiments, currently under way, on alloys should clarify this aspect of the collective mode response.

By using the spectral weight of the combined contribution

$$\int \sigma^*(\nu)d\nu = \frac{c\pi^2}{2}\nu_p^{*2} = \frac{1}{4c}\frac{n^*e^2}{m^*}, \qquad (5)$$

with $n^* = 0.13n$ estimated from the reduction of the magnetic susceptibility [4], we can calculate the effective mass of the collective contribution $m^*/m_b = 40 \pm 10$. This value is in good agreement with the effective mass evaluated just below T_{CDW} [15], further supporting our conclusion that the feature in Fig. 4 is due to the collective mode response. This feature also contributes to σ only along the chain direction, with no such feature perpendicular to the chains.

In conclusion, the experiments reported here give

clear evidence for important deviations from conventional metallic behavior in the fluctuating region, below T_{MF} but above T_{CDW}, the temperature where long range order develops. Our results on the anisotropy clearly establish the collective mode aspect of the conductivity, while the frequency dependence in the direction parallel to the chains give evidence for novel features such as a finite conductivity and a "quasipinned" response. These together with photoemission experiments reported earlier [6] are essential features of the one-dimensional systems when correlations are important. Whether these experiments reflect simply the opening of a pseudogap, or give evidence for non-Fermi liquid behavior remains to be seen. Experiments on alloys, and on $(TaSe_4)_2I$, could further clarify the roles played by fluctuations and impurities in these highly anisotropic materials.

The crystals used in this study were grown by B. Alavi; V.V. Voitsekhovski provided the software for our analysis. The U.S.–Russian collaboration is supported by NSF Grant No. 9216500. We also acknowledge the support of the Russian Research Foundation Grant No. 93-02-16110, and of NSF Grant No. 9218745. One of us (L.D.) would like to thank the Swiss National Science Foundation for financial support of the U.S.–Swiss joint collaboration. M.D. would like to thank the Alexander von Humboldt Foundation for its support.

[1] D.J. Scalapino, Y. Imry, and P. Pincus, Phys. Rev. B **11**, 2042 (1975).

[2] H. Schultz, in *Low Dimensional Conductors and Superconductors*, edited by D. Jérôme and H.R. Caron (Plenum, New York, 1987).

[3] H. Schultz, Int. J. Mod. Phys. **5**, 57 (1991).

[4] D.C. Johnston, Phys. Rev. Lett. **52**, 2049 (1984).

[5] J.P. Pouget and R. Comes, in *Charge Density Waves in Solids*, edited by L.P. Gor'kov and G. Grüner (North-Holland, Amsterdam, 1989).

[6] B. Dardel, M. Malterre, M. Grioni, P. Weibel, Y. Baer, and F. Lévy, Phys. Rev. Lett. **67**, 3144 (1991).

[7] L. Degiorgi, B. Alavi, G. Mihály, and G. Grüner, Phys. Rev. B **44**, 7808 (1991); L. Degiorgi and G. Grüner, Phys. Rev. B **44**, 7820 (1991).

[8] D.S. Perloff, M. Vlasse, and A. World, J. Phys. Chem. Solids **30**, 1071 (1969); C. Schlenker, C. Filippini, J. Marcus, J. Dumas, J.P Pouget, and S. Kagoshima, J. Phys. (Paris), Colloq. **44**, C3-1757 (1983).

[9] O. Klein, S. Donovan, M. Dressel, and G. Grüner, Int. J. Infrared Millimeter Waves **14**, 2423 (1993); S. Donovan, O. Klein, M. Dressel, K. Holczer, and G. Grüner, Int. J. Infrared Millimeter Waves **14**, 2459 (1993); M. Dressel, O. Klein, S. Donovan, and G. Grüner, Int. J. Infrared Millimeter Waves **14**, 2489 (1993).

[10] T. Csiba, A. Blank, M. Dressel, A. Schwartz, G. Grüner, A.A. Volkov, B.P. Gorshunov, and G.V. Kozlov (unpublished).

[11] A.A. Volkov, Yu.G. Goncharov, G.V. Kozlov, S.P. Lebedev, and A.M. Prokhorov, Infrared Phys. **25**, 369 (1985); A.A. Volkov, G.V. Kozlov, and A.M. Prokhorov, Infrared Phys. **29**, 747 (1989).

[12] A.A. Volkov, Yu.G. Goncharov, B.P. Gorshunov, G.V. Kozlov, A.M. Prokhorov, A.S. Prokhorov, V.A. Kozhevnikov, and S.M. Cheshnitskii, Sov. Phys. Solid State **30**, 988 (1988); B.P. Gorshunov, Yu.G. Goncharov, G.V. Kozlov, A.M. Prokhorov, A.S. Prokhorov, and A.A. Volkov, Int. J. Mod. Phys. B **1**, 867 (1987).

[13] L. Degiorgi and G. Grüner, J. Phys. I (France) **2**, 523 (1992); L. Degiorgi, J. Phys. IV (France), Colloq. **3**, C2-103 (1993).

[14] G. Travaglini, P. Wachter, J. Marcus, and C. Schlenker, Solid State Commun. **37**, 599 (1981); G. Travaglini and P. Wachter, Phys. Rev. B **30**, 1971 (1984).

[15] T.W. Kim, D. Reagor, G. Grüner, K. Maki, and A. Virosztek, Phys. Rev. B **40**, 5372 (1989).